

## EXHIBIT D

## Growth suppression by a p14<sup>ARF</sup> exon 1 $\beta$ adenovirus in human tumor cell lines of varying p53 and Rb status

Neshat Saadatmandi, Traci Tyler, Yinghui Huang, Ali Haghighi, Greg Frost,  
Per Borgstrom, and Ruth A Gjerset

Sidney Kimmel Cancer Center, San Diego, California, USA.

We have analyzed the ability of an adenoviral vector encoding the exon 1 $\beta$  region of the p14<sup>ARF</sup> tumor suppressor (ARF) to suppress the growth and viability of an array of tumor cell lines of various origins and varying p53 and Rb status, in order to establish the clinical potential of ARF. An important activity of ARF is regulation of p53 stability and function through binding to the mdm2 protein. By sequestering mdm2, ARF may promote growth suppression through the Rb pathway as well because mdm2 can bind to Rb and attenuate its function. Whereas the high frequency of ARF gene deletion in human cancers, accounting for some 40% of cancers overall, suggests that ARF would be a strong candidate for therapeutic application, the possible dependence of ARF activity on p53 and Rb function presents a potential limitation to its application, as these functions are often impaired in cancer. We show here that a replication-defective adenovirus, Ad1 $\beta$ , encoding the exon 1 $\beta$  region of ARF is most effective in tumor cells expressing endogenous wild-type p53. Nevertheless, Ad1 $\beta$  suppresses tumor cell growth and viability *in vitro* and *in vivo*, inducing G1 or G2 cell cycle arrest and cell death even in tumor cells lacking both functional Rb and p53 pathways, and independently of induction of the p53 downstream targets, p21, bax, and mdm2. These results point to an activity of ARF in human tumor cells that is independent of Rb or p53, and suggest that therapeutic applications based on ARF would have a broad clinical application in cancer.

Cancer Gene Therapy (2002) 9, 830–839 doi:10.1038/sj.cgt.7700505

**Keywords:** p14<sup>ARF</sup>; p53; Rb; tumor suppression; exon 1 $\beta$ ; adenovirus

The ARF tumor suppressor (p14<sup>ARF</sup> in humans, p19<sup>ARF</sup> in mice) is encoded within the INK4a locus on chromosome 9p21 and acts upstream of p53 to regulate its stability and function.<sup>1,2</sup> By interacting with mdm2 and blocking mdm2-mediated degradation of p53,<sup>1–5</sup> ARF enhances sequence-specific transcriptional transactivation by p53<sup>2,4</sup> and restores mdm2-abrogated, p53-mediated cell cycle arrest.<sup>1</sup> The exon 1 $\beta$ -encoded sequence of ARF is the most conserved region between mice and humans, particularly in the first 25 amino acid residues, and is sufficient to inhibit mdm2 activity, stabilize p53, and induce cell cycle arrest.<sup>6</sup> ARF exerts its tumor suppressor activity primarily by enhancing p53 stability and function, but may promote growth suppression through the Rb pathway as well,<sup>7,8</sup> possibly through an effect on mdm2, which has been shown to bind to Rb and inhibit its function.<sup>7</sup>

The importance of ARF for tumor suppression *in vivo* is evident from studies of mice generated through targeted disruption of exon 1 $\beta$ , and therefore lacking ARF function. Such mice are highly cancer-prone and show a phenotype similar to that of mice lacking p53.<sup>4</sup> In human cancer,

ARF gene deletion has now emerged as the second most frequent event in cancer (second to p53 gene alteration), occurring in some 40% of cancers overall.<sup>9–13</sup> ARF and p53 abnormalities have been observed to occur in a reciprocal manner in certain cancers, as would be expected based on the model in which ARF and p53 play roles in the same pathway.<sup>11–13</sup>

Although the high frequency of ARF gene deletion in most human cancers and its involvement in two central pathways of tumor suppression would make ARF a prime candidate for therapeutic application for cancer, the possibility that its tumor suppressor activity requires that either the p53 or Rb pathway be intact is a potential limitation to its application, as these pathways are frequently lost together in cancer. To further understand the interdependence of ARF and p53 in human tumor lines of known endogenous ARF and p53 status, we have examined the response of these cell lines to adenoviral vectors encoding p53 or the exon 1 $\beta$  portion of human ARF (Ad1 $\beta$ ). We find that whereas endogenous p53 status is a strong predictor of cellular response to Ad1 $\beta$ , consistent with the above model, Ad1 $\beta$  is able to suppress the growth and viability of tumors cells lacking endogenous expression of wild-type p53, and lacking a functional Rb pathway as well, inducing partial or complete cell cycle arrest as well as cell death in these cells. The results support a p53-dependent mechanism for ARF, but point to a mechanism for ARF that is independent of p53 as well.

Received May 31, 2002

Address correspondence and reprint requests to: Ruth A Gjerset, Sidney Kimmel Cancer Center, 10835 Alitman Row, San Diego, CA 92121, USA. E-mail: rgjerset@skcc.org

## Materials and methods

### Cell lines and growth conditions

All cell lines except N202 were obtained from the American Type Culture Collection (ATCC, Rockville, MD). An estrogen receptor-negative clone of MCF7 cells derived from the ATCC MCF7 cell line<sup>14</sup> was used in these studies. Murine N202 cells were kindly provided by Dr Joseph Lustgarten (Sidney Kimmel Cancer Center, San Diego, CA) and were originally derived from FVB-neu mice (N202) bearing the rat *neu* protooncogene driven by the mouse mammary tumor virus (MMTV) promoter/enhancer.<sup>15</sup> Such mice are predisposed to spontaneous mammary carcinomas that overexpress the rat p185/neu protein. N202 cells express wild-type p53 and express endogenous ARF (Y Huang, unpublished data). To facilitate *in vivo* detection of N202 cells, they were modified with an expression vector encoding an H2B-Green Fluorescent Protein (GFP) fusion protein (vector kindly provided by Dr Geoffrey Wahl, Salk Institute). All cell lines were maintained at 37 °C in 10% CO<sub>2</sub> in Dulbecco's modified Eagle's medium (DMEM) supplemented with nonessential amino acids, pyruvate, and L-glutamine. Fetal bovine serum (heat-inactivated at 56 °C for 30 minutes) was added to 10%. All media, additives, and serum were obtained from Irvine Scientific (Santa Ana, CA).

### Reverse transcriptase polymerase chain reaction (RT-PCR)

The expression of ARF in various tumor cell lines was determined by RT-PCR using primers designed to amplify a 300-bp fragment of the message encoded by ARF exon 13 (ARF forward: 5'-GATATACTCGAGCTGCTCACCT-3'; ARF exon 13 reverse: 5'-GTATAGGATCCCTGGCTTC-TAGG-3'). Total cellular RNA was prepared from about 5 × 10<sup>7</sup> cells using the RNEasy<sup>®</sup> kit from Qiagen (Valencia, CA) and following the manufacturer's procedure. Five micrograms of RNA was reverse-transcribed into cDNA in a 22-μL reaction containing 0.5 mM each of deoxyribonucleotide triphosphate (dNTP), 50 μg/mL oligo deoxythymidine (oligo-dT), 40 U of rRNasin, 200 U of Moloney Murine Leukemia Virus reverse transcriptase and reverse transcriptase buffer. Control reactions that lacked reverse transcriptase were included, in order to control for the presence of genomic sequences. In all cases, control reactions produced no signal upon PCR amplification. This cDNA was then used as a template for PCR. PCR reactions were performed in 25 μL using 3 μL of cDNA, 25 pmol each of forward and reverse primers, 250 μM each of dNTP (Pharmacia, Piscataway, NJ) 1.25 U of Taq polymerase, 1× buffer, and solution Q (Qiagen), followed by electrophoresis on a 1% agarose gel containing 0.5 μg/mL ethidium bromide. The amplification program was as follows: 1 cycle (94 °C for 1 minute, 30 seconds), 29 cycles (94 °C for 1 minute, 57 °C for 1 minute, 70 °C for 2 minutes, 30 seconds), and 1 cycle (94 °C for 1 minute, 57 °C for 1 minute, 70 °C for 7 minutes). dNTPs for PCR and cDNA preparation were purchased from Pharmacia. Oligo-dT, reverse transcriptase and buffer, and rRNasin were purchased from Promega (Madison, WI). All other PCR reaction components were purchased from Qiagen.

### Western analyses

Cell lysates (50 μg) were electrophoresed on a 15% acrylamide gel and blotted onto PVDF membranes (Osmotics, Minnetonka, MN). Membranes were then treated with primary antibody: p53 (1:500), ARF (1:500), mdm2 (1:500), bax (1:200), and bcl<sub>2</sub> (1:100). Mouse monoclonal anti-p53 (Ab-6) was purchased from Oncogene Research Products (Cambridge, MA). Rabbit polyclonal anti-p14<sup>ARF</sup> (full-length protein) was purchased from Zymed Laboratories (South San Francisco, CA). Mouse monoclonal anti-mdm2 (human) SMP14, rabbit polyclonal anti-bax, mouse monoclonal anti-bcl<sub>2</sub>, mouse monoclonal antiactin, and horse-radish peroxidase-conjugated rabbit IgG and antimouse secondary antibodies were purchased from Santa Cruz Biotechnologies (Santa Cruz, CA). Treatments were carried out according to the protocol recommended by the manufacturer. Antibody reactive bands were revealed using the ECL-Plus Western blotting detection system (Amer sham Biosciences, Piscataway, NJ). For quantitation of bands, we used Kodak digital camera and analysis software (Kodak, Rochester, NY). To control for equivalent loading, blots were stripped and reprobed with antiactin antibody.

### Growth and viability assays

Cells at 60–70% confluence in 24-well plates were treated with adenoviral vectors in a medium containing 2% fetal bovine serum at varying multiplicities of infection and times and then replated in triplicate in 96-well plates at 3000 cells/well (for 72-hour assays) or 1000 cells/well (for 6-day assays) in complete medium. Under these conditions, control (untreated) wells remained subconfluent and in exponential phase growth for the duration of the assay. After 72 hours (in some experiments 6 days), 20 μL of a solution containing 333 μg/mL MTS (3-(4,5'-dimethylthiazol-2-yl)-5-(3-carboxymethoxyphenyl)-2-(4-sulfophenyl)-2H-tetrazolium inner salt) (Promega) and 25 μg/mL PMS (phenazine methosulfate) (Sigma, St. Louis, MO) was added to each well of the 96-well plate. The plate was incubated at 37 °C for approximately 1 hour in a humidified 10% CO<sub>2</sub> atmosphere, and OD at 490 nm, proportional to the number of viable cells, was determined using an ELISA reader. Viability was expressed as a percentage of control, mock-infected cell viability.

### Animal chamber model

Tumor cell spheroids of N202 cells were prepared by placing 150 μL/well of N202 cells (10<sup>5</sup> cells) in DMEM containing 10% fetal bovine serum in 96-well round-bottom plates coated with 1% agarose in serum-free DMEM for a liquid overlay. Plates were incubated at 37 °C in 10% CO<sub>2</sub> for 48 hours. Compacted 100,000-cell spheroids were removed from 96-well plates, washed in serum-free medium, and implanted into the dorsal skinfold chamber of nude mice as previously described.<sup>12,16,17</sup> Intravitreal microscopy was performed using a Mikron fluorescence microscope (Mikron Instruments, San Diego, CA) equipped with an epi-illuminator. A silicon-intensified target camera (SIT68; Dage-MTI, Michigan City, IN) is

attached to the microscope. Visualization of tumor growth in the chamber was achieved using a GFP C 3902 filter cube (Chroma, Battleboro, VT). Cell viability was visualized by the intrinsic fluorescence of H2B-GFP, permitting evaluation of chromatin integrity under  $\times 20$  and  $\times 63$  objectives. Anaphase figures, nuclear karyohexis, and pyknotic nuclei were easily identified under high-power microscopy. Five days following implantation of cells, chambers were injected with  $2 \times 10^8$  pfu of Ad13 or AdLuc, and chambers were observed 24 hours later.

#### Trypan Blue exclusion assay

Duplicate wells of cells in 24-well plates were assayed 48 hours post vector treatment. Medium plus floating cells were removed (1 mL) and the attached cells were detached from the plate with 100  $\mu$ L of 0.05% trypsin in phosphate-buffered saline (PBS), and combined with the medium plus floating cells. A total of 200  $\mu$ L of Trypan Blue stain (0.4% in PBS; Sigma) was added to the cells and the percentage of blue-stained, nonviable cells was determined by cell counting. Averages and standard deviations were calculated.

#### Annexin V staining

Cells were plated in 24-well plates, treated with vector, and stained with Annexin V 24 hours later using the Annexin V apoptosis detection kit (Santa Cruz, Biotechnology, Santa Cruz, CA) according to the manufacturer's instructions. Briefly, the medium was removed and cells were washed once in PBS and once in assay buffer. Cells were then stained by adding 300  $\mu$ L of assay buffer per well, 3  $\mu$ L of Annexin V, and 30  $\mu$ L of propidium iodide. Plates were observed with a fluorescence microscope and photographed immediately.

#### Cell cycle analysis

Cells in 6- or 10-cm culture plates were treated with vector and adherent cells were harvested 48 hours later. Cells were fixed and stained with propidium iodide as previously described.<sup>18</sup> Cell cycle analysis was carried out using a FACScan flow cytometer (Becton Dickinson, Franklin Lakes, NJ). DNA histograms were analyzed with the ModFit program using doublet discrimination. Each analysis was performed in duplicate or triplicate.

#### Adenoviral vectors

A replication-defective adenoviral vector was constructed in which the viral *E1A* and *E1B* genes were replaced with the ARF exon 13 coding sequence, together with the CMV promoter and SV40 polyadenylation signal, using the pE1sp1A and PJM17 plasmids available from Microbix (Toronto, Ontario, Canada). The sequences encoding ARF exon 13 were obtained by PCR amplification from normal human skin fibroblast cDNA, using primers described above (see RT-PCR). Viral packaging was accomplished by cotransfection of human kidney 293 cells (low passage; Microbix) with these two plasmids, followed by overlaying the cells with complete medium containing 1% agarose and

incubating at 37°C in 10% CO<sub>2</sub> until plaques appeared (about 3 weeks). The virus was isolated from these plaques, expanded, and purified on cesium chloride gradients using published procedures<sup>19</sup> and characterized for the ability to induce expression of ARF exon 13 in the ARF-negative cell line MCF7, as determined by RT-PCR and Western analysis. Viral titers in viral particles (vp) per milliliters were determined by measuring the OD 260 nm and calculating concentration based on the relationship: 1 OD(260) =  $10^{12}$  vp/mL. Viral titers in plaque-forming units per milliliter (pfu/mL) were determined by an endpoint dilution assay on 293 cells in 96-well plates as described for the TCID<sub>50</sub> assay in the Quantum Biotechnologies AdEasy<sup>®</sup> applications manual (Quantum Biotechnologies, Carlsbad, CA), and found to be  $10^{11}$  pfu/mL. The vp-to-pfu ratio was 70. Replication-competent virus was not detectable in  $10^{10}$  vp assayed on human fibroblasts.

Replication-defective adenoviral vectors encoding human wild-type p53 (RPR/INGN201, Ad5CMV-p53), firefly luciferase, and bacterial 3-galactosidase were provided by Introgen Therapeutics (Houston, TX).<sup>20,21</sup> These are referred to here as Adp53, AdLuc, and Adβgal, respectively, and have been used previously in our studies.<sup>22</sup> The p53 and β-galactosidase genes are expressed from the Cytomegalovirus promoter. The luciferase gene is expressed from the Rous Sarcoma Virus promoter. All vectors are E1A- and E1B-deleted. Viral titers were as follows: Adp53:  $3.6 \times 10^{10}$  pfu/mL; AdLuc:  $2 \times 10^{11}$  pfu/mL; and Adβgal:  $10^{11}$  pfu/mL. The vp-to-pfu ratios were about 50–80 for all three vectors.

#### X-gal staining

To assess the efficiency of adenoviral infection in each cell line, cells were treated with varying doses of Adβgal for 3 hours, and 48 hours following vector treatment, cells were fixed in 3.7% formaldehyde in PBS and stained with the β-galactosidase substrate X-gal (5-bromo-4-chloro-3-indol-3-β-D-galactopyranoside), which generates a blue-colored product in cells expressing the transduced β-galactosidase gene, as previously described.<sup>18</sup>

#### Results

##### Frequent reciprocity of ARF and p53 abnormalities in human tumor cell lines

We investigated by RT-PCR, the ARF status in a panel of 17 human tumor cell lines of known p53 status (Table 1). p53 abnormalities occurred in 14 of 17 cell lines examined, with a reciprocal relationship between ARF and p53 abnormalities occurring in 13 of 17 cell lines. Three cell lines, T98G glioblastoma, U373 glioblastoma, and SKOV3 ovarian carcinoma, had abnormalities in both p53 and ARF. LnCAP prostate cancer cells expressed ARF, which we confirmed by sequence analysis to correspond to the published wild-type sequence<sup>23</sup> (data not shown) and to retain wild-type p53 (confirmed by sequence analysis; data not shown). As shown below, LnCAP cells do not appear to overexpress mdm2 protein, the other key modulator of p53 stability and function, and thus appear to have the p53 pathway intact.

**Table 1** p53 and ARF status of tumor cell lines

Cell line	p53 status (see last column)	ARF status*	Reciprocal events?	Reference for p53 status
<i>Breast cancer</i>				
MCF7	Wild type	Negative		[46]
T47D	Mutant	Positive		†
MDA-MB-435	Mutant	Positive		[47]
MDA-MB-231	Mutant	Positive		†
N202 (murine)	Wild type	Positive		‡
<i>Glioblastoma</i>				
T98G	Mutant	Negative	No	†
U87	Wild type	Negative		[48]
U373	Mutant	Negative	No	
<i>Lung cancer</i>				
H23 (sccl)	Mutant	Positive		†
H358 (nsclc)	Null	Positive		[49]
<i>Head/neck cancer</i>				
FaDu	Mutant	Positive		†
<i>Colon cancer</i>				
HT29	Mutant	Positive		†
SW480	Mutant	Positive		†
<i>Ovarian cancer</i>				
SKOV3	Null	Negative	No	[50]
<i>Osteosarcoma</i>				
SaOS-2	Null	Positive		[51]
<i>Prostate cancer</i>				
PC-3	Null	Positive		†
DU145	Mutant	Positive		†
LncAP	Wild type	Positive	No	†

\*Determined by RT-PCR.

†See <http://www.iarc.fr/p53/Index.html>.

‡Y Huang (data not shown).

The N202 murine breast cancer cell line also expressed ARF and retained expression of wild-type p53 (confirmed by sequence analysis; data not shown).

#### Broad tumor suppressor activity of Ad13 in human tumor cell lines

We constructed an E1A/E1B-deleted replication-defective adenovirus, denoted Ad13, encoding the exon 13 portion of ARF — the region demonstrated to encode ARF tumor suppressor activity.<sup>1</sup> The tumor suppressor activity of Ad13 was verified using the MCF7 cell line that lacks endogenous ARF (Fig 1A, lane a) and expresses endogenous wild-type p53 (see Table 1). We observed that MCF7 cells treated with Ad13 underwent a dose-dependent increase in immunoreactive protein corresponding to ARF exon 13 (Fig 1A, lanes b and c) that correlated inversely with the viability of Ad13-treated cultures (Fig 1B). Viability was measured by the MTS assay (described in *Materials and methods*) 72 hours following the start of treatment. The term viability is used throughout this study to mean the overall metabolic activity of the cell population as reflected by the bioconversion of a

tetrazolium salt, MTS, to a colored product, and is proportional to the cell number. Suppression of viability refers to the percent decrease in overall metabolic activity of the vector-treated cell population relative to an untreated population. Equivalent loading on Western blots was verified by stripping the blots and reprobe with actin antibody (not shown). No suppression of viability was observed in AdLuc-treated cultures (Fig 1B), indicating that nonspecific vector-associated toxicity was undetectable.

As shown in Figure 2, A and B, respectively, Ad13 also suppressed the *in vitro* viability and *in vivo* tumorigenicity of murine N202 cells, which express endogenous wild-type p53 as well as endogenous ARF (Table 1). Treatment of N202 cells with 200 pfu/cell Ad13 for 3 hours resulted in 12±2% Trypan Blue-stained cells, 48 hours after vector treatment, indicating that cell death occurred. Control vector-treated cells had no detectable staining. For visualization of *in vivo* effects, we used intravitral video microscopy of tumor cell spheroids implanted in dorsal skinfold chambers in nude mice<sup>14,16,17</sup> followed by treatment with Ad13 or AdLuc (control). To distinguish apoptosis from mitotic arrest, tumor cells had been modified *ex vivo* to

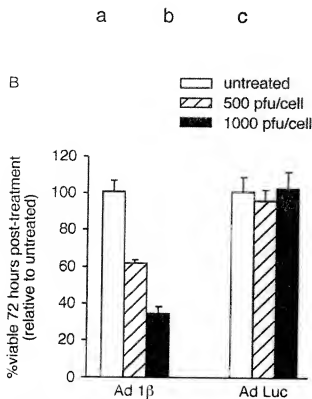


**Figure 1 A:** Induction of immunoreactive ARF exon 13 protein 48 hours following treatment of MCF7 cells with Ad13. Cell lysates were prepared from untreated cells (**lane a**), and from cells 48 hours following treatment for 3 hours with 500 pfu/cell Ad13 (**lane b**) or 1000 pfu/cell Ad13 (**lane c**). Each lane corresponds to 50 µg of cellular protein. **B:** Average viability based on triplicate assays of MCF7 cells 72 hours following the indicated vector treatments. Viability (see text for definition) is expressed as a percentage of the viability measured for untreated cells.

constitutively express a Histone H2B-GFP fusion protein, a fluorescent marker protein that localizes to the chromatin and enables visualization of nuclear morphology. Murine N202 cells grow as a nonencapsulated tumor resembling a spontaneous tumor, unlike the majority of human tumor lines, including MCF7, in a murine environment (P Borgstrom, unpublished data), and they therefore allow us to assess the behavior of tumor cells in a growth environment more closely resembling a clinical situation. Five days following implantation,  $2 \times 10^8$  pfu of Ad13 or AdLuc (control) was injected into the chamber, and the cellular response was observed 24 hours later. As shown in Figure 2B, treatment with Ad13 (Right panel), but not AdLuc (Left panel), led to a striking increase in cells with condensed and irregular nuclei characteristic of apoptotic cells. Therefore, Ad13 encodes an immunoreactive exon 13 protein with tumor suppressor function in both murine and human tumor cells and with activity both *in vitro* and *in vivo*.

To determine whether the tumor suppressor activity of Ad13 extended to human tumor cell lines of varying p53

and ARF status, we selected seven representative cell lines from those listed in Table I. The cell lines (Table 2) were chosen so as to represent each of the four possible states of p53 and ARF status: (a) abnormal p53 only (DU145, PC3); (b) abnormal ARF only (MCF7, U87); (c) abnormal p53 and ARF (T98G, SKOV3); and (d) wild-type p53 and ARF (LnCAP). In addition, with the exception of LnCAP cells, all cell lines tested lacked expression of either Rb or p16, and therefore lacked a functional Rb pathway.<sup>24-30</sup>

The relative infectabilities of cell lines were variable, as determined 48 hours following treatment of cells with an adenoviral vector (Ad3gal) expressing the bacterial  $\beta$ -galactosidase gene (see Materials and Methods). Nevertheless, conditions that ensured a high percentage of transduced cells (>80%) in all cases based on X-gal staining could be found, and were as follows: 500–1000 pfu/cell, overnight (T98G, SKOV3); 500 pfu/cell, 3 hours (PC3); 200–500

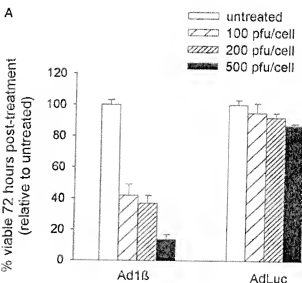


**Figure 2 A:** Percent viability (relative to untreated cells) of N202 cells 72 hours after treatment with the indicated vector doses (average of triplicate assays). **B:** Photomicrograph illustrating the effect of Ad13 treatment of N202 tumor cells in dorsal skinfold chamber in nude mice. N202 cells were modified to express a histone H2B-GFP fusion protein in order to visualize nuclear events. **B: Left panel:** Control chamber treated with  $2 \times 10^8$  pfu of AdLuc and examined 24 hours later. Diffuse nuclear staining of interphase nuclei is evident in most cells. One mitotic cell is indicated by the arrow. **Right panel:** Chamber treated with  $2 \times 10^8$  pfu of Ad13 and examined 24 hours later. A large fraction of cells shows condensed and fragmented nuclei typical of apoptotic cells, several of which are indicated by arrows. Magnification  $\times 200$ .

**Table 2** Summary of relative suppression by Adp53 and Ad13

Cell line	Status		Suppression
	p14*	p53	
SKOV3	—	—	p53>>13
PC3	+	—	
T98G	—	m	p53>13
DU145	+	m	
LnCAP	+	wt	1.3±p53
MCF7	—	wt	
U87	—	wt	

\*Determined by RT-PCR. m=mutant; wt=wild type.

pfu/cell, 3 hours (DU145, MCF7); and 100–200 pfu/cell, 3 hours (LnCAP, U87).

These cell lines were then treated with varying doses of Ad13, Adp53, or AdLuc (control), and cell viability was measured as for Figure 1 (see also Materials and Methods) 72 hours following the start of treatment (Fig 3). Vector treatment also resulted in a reduction in [<sup>3</sup>H]thymidine incorporation into DNA that paralleled the results of the MTS assay (data not shown). The results show that nonspecific vector-associated toxicity was minimal, as the AdLuc control vector was well tolerated by the lines under all conditions. Because all three viral preparations displayed similar vp-to-pfu ratios (in the range of 50–80), nonspecific vector-associated toxicity was assumed to be similar for all three vectors.

We observed that suppression of viability (defined above) by Adp53 was independent of endogenous ARF and p53 status, as expected, and reached >95% for all cell lines tested. Suppression of 72-hour viability by Ad13 fell into one of three patterns that depended on endogenous p53 status: (a) cell lines null for endogenous p53 expression (SKOV3, PC-3) were not suppressed by Ad13 (Fig 3A, column 1; Table 2); and (b) cell lines expressing endogenous mutant p53 (T98G, DU145) were less suppressed by Ad13 than they were by Adp53 at equivalent vector doses (Fig 3A, column 1; Table 2). At the highest treatment dose of Ad13, T98G and DU145 could be suppressed by about 50% and >95%, respectively, with data points being completely nonoverlapping with controls. Finally, (c) three cell lines expressing endogenous wild-type p53 (LnCAP, MCF7, U87) were suppressed by both Adp53 and Ad13 to similar extents at equivalent vector doses (Fig 3A, column 2; Table 2). In one cell line null for endogenous p53 (PC-3), growth and viability could be suppressed by about 25% by 6 days posttreatment (Fig 3B). Thus, expression of endogenous wild-type p53 contributes to Ad13-mediated suppression of tumor cell growth and viability, but is not strictly required. Furthermore, because T98G cells lack expression of the cyclin-dependent kinase inhibitor, p16,<sup>27</sup> and therefore have a defective Rb pathway, and DU145 cells express a nonfunctional Rb protein,<sup>30</sup> these results suggest an activity of ARF in human tumor cell lines that is independent of either the p53 or Rb pathway.

### Induction of cell death and cell cycle arrest in Ad13-treated cells in the absence of induction of p53 downstream targets

To determine the extent to which cell death or cell cycle arrest accounted for the Ad13-mediated decrease in overall culture viability observed in Figure 3, we performed quantitative Trypan Blue exclusion assays of total cell death, Annexin V staining assays of apoptotic cell death, and Flow Cytometric analyses of cell cycle changes 24–48 hours after vector treatment of four representative cell lines (T98G, DU145, LnCAP, U87). Vector treatments were chosen based on Figure 3 to provide about 50–70% suppression of the 72-hour viability: (a) 500 pfu/cell, overnight (Ad13, AdLuc) and 500 pfu/cell, 3 hours (Adp53) for T98G and DU145; (b) 200 pfu/cell, 3 hours (all vectors) for LnCAP; and (c) 500 pfu/cell, 3 hours (all vectors) for U87.

Trypan Blue staining, which measures cellular membrane breakdown characteristic of total cell death (apoptotic+nonapoptotic), was carried out in duplicate 48-hour post-vector treatment. In control vector (AdLuc)-treated cells, viability was high and Trypan Blue-stained cells accounted for only a small percentage of the population: 1±2% (T98G), 0±0% (DU145), 1±1% (LnCAP), and 6±2% (U87). In all four Adp53-treated cell lines (irrespective of endogenous p53 status), there was a marked increase in Trypan Blue staining relative to control vector-treated cells: 17±5% (T98G), 37±5% (DU145), 29±3% (LnCAP), and 36±1% (U87), as expected. In three of four cell lines (DU145, LnCAP, U87), Ad13 treatment also led to a marked increase in Trypan Blue staining: 13±6% (DU145), 29±3% (LnCAP), and 36±1% (U87). One of these cell lines (DU145) expressed endogenous mutant p53, indicating that Ad13 did not require endogenous wild-type p53 expression to induce cell death.

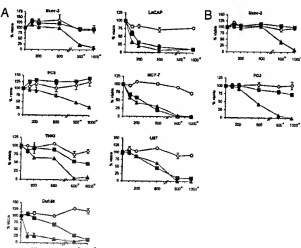


**Figure 3** Percent viability (relative to untreated cells) of human tumor cell lines measured at (A) 72 hours, or (B) 6 days after treatment of cells with the indicated doses of AdLuc, Ad13, or Adp53. Doses (x axis) are shown as pfu per cell for 3 hours or overnight (overnight treatments indicated by asterisks). Viability was determined as in Figures 1 and 2A. Each data point represents the average of triplicate samples, with standard deviations shown. Each assay was repeated on at least one additional occasion, with similar results. Symbols are as follows: (○) AdLuc, (▲) Adp53, (■) Ad13.

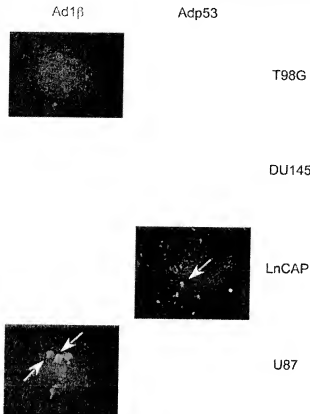


**Figure 4** Annexin V staining patterns on T98G, DU145, LnCAP, and U87 cells 24 hours following treatment with Ad1 $\beta$  or Adp53 at doses described in text. Fields were chosen so as to avoid scoring permeabilized cells (propidium iodide-positive). Such cells represented less than 1% of the cell population. Arrows indicate some of the typical Annexin V-stained cells. Magnification  $\times 100$ .

We used Annexin V–FITC binding to cells 24 hours after vector treatment to detect the early phases of apoptosis in live, intact cells prior to membrane permeabilization (Fig 4). At this early stage, membrane-permeable cells (detected by propidium iodide staining) accounted for less than 1% of the cell population (not shown) and these were not scored for Annexin staining. Figure 4 shows typical Annexin staining patterns of T98G, DU145, LnCAP, and U87 cells following treatment with either Ad1 $\beta$  or Adp53. Annexin staining was not observed in control cultures or in cultures treated with AdLuc (not shown). Annexin staining could be observed in all cell lines following treatment with Adp53, indicating that apoptosis was triggered by the treatment, and consistent with an elevated bax-to-bcl<sub>2</sub> ratio observed by Western analysis (see below). Following treatment with Ad1 $\beta$ , LnCAP cells and U87 cells that express endogenous wild-type p53 displayed Annexin staining, whereas T98G cells and DU145 cells that lack endogenous expression of wild-type p53 failed to display Annexin staining. Together with the results of the Trypan Blue Exclusion assay, these data suggest that apoptosis is not efficiently triggered by Ad1 $\beta$  unless cells express endogenous wild-type p53. However, even when apoptosis is not detected, a nonapoptotic form of cell death may contribute to the loss of viability observed after Ad1 $\beta$

treatment of some cell lines lacking endogenous expression of wild-type p53.

We used FACS analysis to examine cell cycle changes 48 hours following treatment with Ad1 $\beta$  or Adp53 (Fig 5). We found that Adp53 treatment induced an accumulation of cells with G1 DNA content in all four cell lines. Ad1 $\beta$  treatment induced an accumulation of cells with G1 DNA content (LnCAP, G2 DNA content (U87), or S/G2 DNA content (DU145), and the arrest pattern could not be predicted from the endogenous p53 status of the cells. That is, U87 cells that expressed endogenous wild-type p53 were arrested in G1 by Adp53, and G2 by Ad1 $\beta$ . Taken together, the results of the Trypan Blue exclusion assay, the Annexin V staining assay, and the cell cycle analysis reveal differences in Ad1 $\beta$ - and Adp53-treated cells, which suggest that the pathways induced by the two vectors are, in part, different.

#### Western analysis of p53 target genes

We used Western blotting to examine the expression of the p53 target gene *bax*, known to be associated with apoptosis, in cell lysates prepared 72 hours after treatment with Ad1 $\beta$  or Adp53. Induction of mdm2, a p53 target involved in feedback regulation of p53 stability, and of p21, a p53 target involved in cell cycle arrest, was also examined. We also examined the expression of *bcl<sub>2</sub>* and calculated the bax-to-bcl<sub>2</sub> ratio, a critical determinant of apoptosis. All cell lines except LnCAP were treated with 500 pfu/cell vector for 3 hours. LnCAP cells were treated with 200 pfu/cell vector for 1 hour.

As shown in Figure 6 (first and second rows), treatment of all cell lines with Adp53 resulted in an increase in p53 protein, and treatment of cells with Ad1 $\beta$  resulted in an increase in exon 1.3 protein, as expected. Endogenous levels

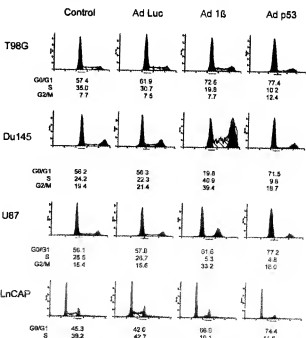


**Figure 5** FACS analysis of propidium iodide-stained cells treated as described in text and harvested 48 hours posttreatment.

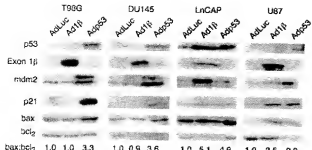


**Figure 6** Western blot analysis of p53, exon 13, mdm2, bax, and bcl<sub>2</sub> expression in T98G, DU145, LnCAP, and U87 cells following treatment with AdLuc (control), Ad13, or Adp53, as described in the text. The expression of bax and bcl<sub>2</sub> was quantitated using a Kodak camera and analysis software and the ratios of bax to bcl<sub>2</sub> following treatment with each vector are shown in the last row, after normalizing the ratios to that of Ad13-treated cells. Each lane represents 50 µg of protein. Equivalent loading was verified by stripping membranes and reprobing with actin antibody (not shown).

of p53 and ARF were low to undetectable under our conditions. In all cell lines treated with Adp53, expression of p53 target genes mdm2 (third row), p21 (fourth row), and bax (fifth row) was also induced relative to levels in AdLuc-treated cells, and an increased bax-to-bcl<sub>2</sub> ratio indicative of induction of p53-mediated apoptosis was observed (bottom row). A second analysis of bax-to-bcl<sub>2</sub> ratios in independently prepared lysates gave similar results (not shown). The doublet band observed for mdm2 in T98G, DU145, and LnCAP cells may represent differentially phosphorylated forms or the products of multiple transcripts.<sup>51</sup> In cell lines expressing endogenous wild-type p53 (LnCAP and U87), treatment with Ad13 led to increased levels of endogenous p53, consistent with the involvement of ARF in the p53-mdm2 feedback loop, and resulted in increased expression of p53 downstream targets. Thus, expression of exon 13 triggered the p53 pathway in these cells.

In contrast, Ad13 treatment of T98G and DU145 cells that lack endogenous wild-type p53 expression did not result in increased expression of p53 or its downstream target genes. As shown in Figure 6, levels of mdm2, p21, and bax following treatment of T98G or DU145 cells with Ad13 were similar to levels observed following treatment with control vector (AdLuc). Bax-to-bcl<sub>2</sub> ratios in Ad13-treated T98G and DU145 cells were also similar to ratios observed in control vector (AdLuc)-treated cells. Lysates from T98G cells treated overnight with 500 pfu/cell Ad13 (not shown) gave results similar to those shown for 500 pfu/cell for 3 hours.

## Discussion

This study examined the suppressive effects of a p14<sup>ARF</sup> exon 13 adenovirus (Ad13) in human tumor cell lines of varying endogenous p53 and ARF status, so as to address the possible application of ARF-based therapies to the treatment of cancer. The high frequency with which the ARF gene is deleted in human cancer makes ARF a promising candidate for therapy. However, the possibility that efficient tumor

suppression by ARF would require an intact p53 and/or Rb pathway raises a concern as to the generality of its application. We show that Ad13 is most effective in cell lines expressing endogenous wild-type p53. Ad13 has little to no activity in two cell lines that are null for endogenous p53 expression (SKOV3, PC-3). However, Ad13 has tumor suppressor activity, as manifested by the induction of cell cycle arrest and/or cell death, in two human tumor cell lines expressing endogenous mutant p53 (T98G, DU145). Because these lines cells also lack a functional Rb pathway, the results point to an activity of ARF that is independent of p53 and Rb in these settings, through a mechanism that is unknown. Suppression of tumor cell growth and viability following treatment with Ad13 involves both the induction of cell death and cell cycle arrest. Induction of apoptosis by Ad13, determined by Annexin V staining of vector-treated cells, is observed only in cells expressing endogenous wild-type p53.

Cell cycle analyses, Trypan Blue exclusion assays for cell death, and Annexin V staining assays of vector-treated cells pointed to both p53-dependent and -independent activities of ARF. Thus, whereas apoptosis induction by Ad13 occurred only in cell lines expressing endogenous wild-type p53 (LnCAP, U87), induction of an apparently nonapoptotic form of cell death by Ad13, revealed by Trypan Blue staining, could be observed in DU145 cells that express endogenous mutant p53. In addition, the cell cycle distribution observed in cells treated with Ad13 or Adp53 did not necessarily follow a pattern predicted from a model in which ARF acts entirely through the p53 pathway. Thus, Ad13 induced an accumulation of cells in G2 in U87 cells expressing endogenous wild-type p53, whereas Adp53 induced an accumulation of cells in G1 in these cells.

We used Western blot analysis of four representative cell lines (T98G, DU145, LnCAP, U87) to examine the p53 downstream targets mdm2, p21, and bax, whose promoters are induced by p53. As expected, induction of these targets by Ad13 required that the cell express endogenous wild-type p53 (LnCAP, U87). Furthermore, Ad13 treatment induced an elevated bax-to-bcl<sub>2</sub> ratio characteristic of apoptosis only in cells expressing endogenous wild-type p53 (LnCAP, U87), consistent with the Annexin V staining results. In contrast, Adp53 treatment induced these genes and resulted in an elevated bax-to-bcl<sub>2</sub> ratio in all four cell lines irrespective of endogenous p53 and ARF status. The results are consistent with wide range of studies showing that an important activity of ARF is induction of the p53 pathway. However, the fact that suppression of viability by Ad13 occurs in cells lacking endogenous p53, and in the absence of induction of the p53 pathway, points to additional pathways of suppression of ARF as well.

Numerous lines of evidence support a model in which p53 and ARF have interdependent roles. For example, p53-mediated apoptosis in the developing lens of Rb<sup>-/-</sup> mice is attenuated in the absence of ARF expression.<sup>52</sup> And, whereas γ-radiation-induced phosphorylation, stabilization, and accumulation of p53 occur in the absence of ARF,<sup>4</sup> the duration of that response is shortened in the absence of ARF expression.<sup>53</sup> Conversely, in some settings, ARF function depends on p53: ARF does not induce growth arrest of early passage mouse embryo fibroblasts (MEFs) nullizygous for

p53.<sup>2,4,5,3</sup> Suppression of transformation of rat fibroblasts by ARF also requires expression of wild-type p53.<sup>2</sup>

Nevertheless, it is becoming increasingly clear that the functions of ARF and p53 are not entirely interdependent. A reciprocal relationship between ARF loss and p53 mutation has not been observed in all cancers, for example,<sup>34,35</sup> suggesting that inactivation of ARF *per se* may constitute an independent survival advantage for the cancer cell. Moreover, triple knockout mice nullizygous for p53, mdm2, and ARF display a broader spectrum of tumors that develop more rapidly compared to double knockout mice lacking only p53 and mdm2, or single knockout mice lacking only p53, indicating that ARF expression in single or double knockout mice reduces tumor formation. In one study, MEFs from mice nullizygous for p53, mdm2, and ARF were observed to be growth-suppressed by ectopic reexpression of ARF, indicating that ARF is able to suppress cell growth independently of p53 in some cases.<sup>36</sup> Another study reported that immortalized MEFs from p53 nullizygous mice could be growth-suppressed by ectopic expression of ARF, whereas inactivation of both the p53 and Rb pathways effectively abrogated growth suppression by ARF.<sup>8</sup> These results reveal a more complex pattern of suppression by ARF and p53 — one that might not be predicted simply on the basis of endogenous p53 and ARF status. In the present study, Ad13-mediated suppression of T98G and DU145 cannot be explained by an absence of mdm2 expression, as mdm2 was readily detected in these cells, or by an Rb pathway-mediated effect, as both cell lines had defects in this pathway. ARF has now been found to interact with several proteins in addition to mdm2, including E2F-1,<sup>37</sup> topoisomerase,<sup>38</sup> and mdmx,<sup>39</sup> and these or other proteins may play roles in ARF activity in certain human tumor cells. One possibility, though speculative, is that an interaction of ARF with the DNA replicative machinery could disrupt mitosis and lead to cell death through nonapoptotic and p53-independent mitotic catastrophe.

The tumor suppressor activity of an adenoviral vector encoding full-length ARF has been evaluated in cell lines derived from mesothelioma, a cancer characterized by frequent deletions of the INK4A locus and rare mutations of p53. In that study, mesothelioma cell lines lacking expression of ARF and expressing wild-type p53 were markedly growth-suppressed and underwent apoptosis following treatment with a ARF adenovirus, an observation that supports the therapeutic application of ARF gene therapy for that disease.<sup>40</sup> Our results with an adenoviral vector encoding only the exon 13 portion of ARF are consistent with this study, and suggest in addition that the therapeutic application of ARF may extend to a broader range of tumors lacking wild-type p53, or lacking both wild-type p53 and Rb pathways.

Therapeutic applications of the p53 tumor suppressor are already in an advanced stage of development, with numerous clinical trials ongoing or completed that attest to the safety and efficacy of adenovirus-mediated p53 gene transfer in cancer patients.<sup>41–45</sup> Because ARF-based therapies may be highly effective in certain cancers and involve, in part, pathways that are independent of p53, an extension of these clinical approaches to include ARF gene transfer seems

feasible, and potentially promising for many cancers. A better understanding of the tumor suppressor activity of ARF, particularly the activity that is independent of p53, may also reveal new opportunities for therapeutic intervention.

### Acknowledgments

This work was supported by Grants (RAG) from the California Cancer Research Program (no. 99-00517V-10140), the California Breast Cancer Research Program (no. 6JB-0077), the Department of Defense Breast Cancer Research Program (no. DAMD 17-96-1-6038), and the National Cancer Institute (no. CA69546).

### References

- Zhang Y, Xiong Y, Yarbrough WG. ARF promotes MDM2 degradation and stabilizes p53: ARF-INK4a locus deletion impairs both the Rb and p53 tumor suppression pathways. *Cell*. 1998;92:725–734.
- Pomerantz J, Schreiber-Agus N, Liegeois NJ, et al. The Ink4a tumor suppressor gene product, p19Arf, interacts with Mdm2 and neutralizes Mdm2's inhibition of p53. *Cell*. 1998;92:713–723.
- Kamijo T, Weber JD, Zambetti G, et al. Functional and physical interactions of the ARF tumor suppressor with p53 and Mdm2. *Proc Natl Acad Sci USA*. 1998;95:8292–8297.
- Kamijo T, Zindy F, Roussel MF, et al. Tumor suppression at the mouse Ink4a locus mediated by the alternative reading frame product p19ARF. *Cell*. 1997;91:649–659.
- Honda R, Yasuda H. Association of p19(ARF) with Mdm2 inhibits ubiquitin ligase activity of Mdm2 for tumor suppressor p53. *EMBO J*. 1999;18:22–27.
- Rizos H, Darmanian AP, Mann GJ, et al. Two arginine rich domains in the p14ARF tumor suppressor mediate nucleolar localization. *Oncogene*. 2000;19:2979–2985.
- Xiao ZX, Chen J, Levine AJ, et al. Interaction between the retinoblastoma protein and the oncoprotein MDM2. *Nature*. 1995;375:694–698.
- Carnero A, Hudson JD, Price CM, et al. p16INK4A and p19ARF act in overlapping pathways in cellular immortalization. *Nat Cell Biol*. 2000;2:148–155.
- Haber DA. Splicing into senescence: the curious case of p16 and p19ARF. *Cell*. 1997;91:555–558.
- Vonlanthen S, Heighway J, Tschan MP, et al. Expression of p16INK4a/p16alpha and p19ARF/p16beta is frequently altered in non-small cell lung cancer and correlates with p53 overexpression. *Oncogene*. 1998;17:2779–2785.
- Kannan K, Munirajan AK, Krishnamurthy J, et al. The p16INK4a/alpha-p19ARF gene mutations are infrequent and are mutually exclusive to p53 mutations in Indian oral squamous cell carcinomas. *Int J Oncol*. 2000;16:585–590.
- Piryol M, Hernandez L, Martinez A, et al. INK4a/ARF locus alterations in human non-Hodgkin's lymphomas mainly occur in tumors with wild-type p53 gene. *Am J Pathol*. 2000;156:1987–1996.
- Fuleki G, Labuhn M, Maier D, et al. p53 gene mutation and ink4a/arf deletion appear to be two mutually exclusive events in human glioblastoma. *Oncogene*. 2000;19:3816–3822.
- Borgstrom P, Gold DF, Hillan KJ, et al. Importance of VEGF for breast cancer angiogenesis *in vivo*: implications from intravital microscopy of combination treatments with an anti-VEGF

- neutralizing monoclonal antibody and doxorubicin. *Anticancer Res.* 1999;19:4203–4214.
- Sacco MG, Gribaldo L, Barbieri O, et al. Establishment and characterization of a new mammary adenocarcinoma cell line derived from MMTV neu transgenic mice. *Breast Cancer Res Treat.* 1998;47:171–180.
  - Torres Filho IP, Hartley-Asp B, Borgstrom P. Quantitative angiogenesis in a syngeneic tumor spheroid model. *Microvasc Res.* 1995;49:212–226.
  - Lehr HA, Leuning M, Menger MD, et al. Dorsal skinfold chamber technique for intravital microscopy in nude mice. *Am J Pathol.* 1993;143:1055–1062.
  - Gjerset RA, Turla ST, Sobol RE, et al. Use of wild-type p53 to achieve complete treatment sensitization of tumor cells expressing endogenous mutant p53. *Mol Carcinog.* 1995;14:275–285.
  - Gruhnn FL, Prevec L. Manipulations of adenovirus vectors. In: Murray J, ed. *Methods in Molecular Biology*. New Jersey: Humana Press; 1991.
  - Zhang WW, Fang X, Brinch CD, et al. Generation and identification of recombinant adenovirus by liposome-mediated transfection and PCR analysis. *Biotechniques.* 1993;15:868–872.
  - Ghaneh P, Greenhalf W, Humphreys M, et al. Adenovirus-mediated transfer of p53 and p16INK4a results in pancreatic cancer regression *in vitro* and *in vivo*. *Gene Ther.* 2001;8:199–208.
  - Lebedeva S, Bagdasarova S, Tyler T, et al. Tumor suppression and therapy sensitization of localized and metastatic breast cancer by adenovirus p53. *Hum Gene Ther.* 2001;12:763–772.
  - Stone S, Jiang P, Dayanantis P, et al. Complex structure and regulation of the P16 (MTS1) locus. *Cancer Res.* 1995;55:2988–2994.
  - Costanzi-Strauss E, Strauss BE, Naviaux RK, et al. Restoration of growth arrest by p16INK4a/p21WAF1/pRB, and p53 is dependent on the integrity of the endogenous cell-cycle control pathways in human glioblastoma cell lines. *Exp Cell Res.* 1998;238:51–62.
  - Parry D, Bates S, Mann DJ, et al. Lack of cyclin D-Cdk complexes in Rb-negative cells correlates with high levels of p16INK4/MTS1 tumour suppressor gene product. *EMBO J.* 1995;14:503–511.
  - Zhao X, Day ML. RB activation and repression of C-MYC transcription precede apoptosis of human prostate epithelial cells. *Urology.* 2001;57:860–865.
  - Higashii H, Suzuki-Takahashi I, Yoshida E, et al. Expression of p16INK4a suppresses the unbounded and anchorage-independent growth of a glioblastoma cell line that lacks p16INK4a. *Biochem Biophys Res Commun.* 1997;231:743–750.
  - Jarrard DF, Bova GS, Ewing ML, et al. Deletional, mutational, and methylation analyses of CDKN2 (p16/MTS1) in primary and metastatic prostate cancer. *Genes Chromosomes Cancer.* 1997;19:90–96.
  - Schultz DC, Vanderveer L, Buetow KH, et al. Characterization of chromosome 9 in human ovarian neoplasia identifies frequent genetic imbalance on 9q and rare alterations involving 9p, including CDKN2. *Cancer Res.* 1995;55:2150–2157.
  - Steiner MS, Wang Y, Zhang Y, et al. p16/MTS1/INK4a suppresses prostate cancer by both pRB dependent and independent pathways. *Oncogene.* 2000;19:1297–1306.
  - Guida JM, Nguyen H, Klein RC, et al. Differential expression of multiple MDM2 messenger RNAs and proteins in normal and tumorigenic breast epithelial cells. *Clin Cancer Res.* 1995;1:71–80.
  - Khan SH, Moritzuji G, Wahl GM. Differential requirement for p19ARF in the p53-dependent arrest induced by DNA damage, microtubule disruption, and ribonucleotide depletion. *Proc Natl Acad Sci USA.* 2000;97:3266–3271.
  - Stott EJ, Bates S, James MC, et al. The alternative product from the human CDKN2A locus, p14(ARF), participates in a regulatory feedback loop with p53 and MDM2. *EMBO J.* 1998;17:5001–5014.
  - Sanchez-Cespedes M, Reed AL, Buta MJ, et al. Inactivation of the INK4A/ARF locus frequently coexists with TP53 mutations in non-small cell lung cancer. *Oncogene.* 1999;18:5843–5849.
  - Gazzeri S, Della Valle V, Chaussade L, et al. The human p19ARF protein encoded by the beta transcript of the p16INK4a gene is frequently lost in small cell lung cancer. *Cancer Res.* 1998;58:3926–3931.
  - Weber JD, Jeffers JR, Rehg JE, et al. p53-independent functions of the p19(ARF) tumor suppressor. *Genes Dev.* 2000;14:2358–2365.
  - Eymim B, Karayan L, Seite P, et al. Human ARF binds E2F1 and inhibits its transcriptional activity. *Oncogene.* 2001;10:1033–1041.
  - Karayan L, Riou JJ, Seite P, et al. Human ARF protein interacts with Topoisomerase I and stimulates its activity. *Oncogene.* 2001;19:836–848.
  - Jackson MW, Lindsstrom MS, Berberich SJ. MdmX binding to ARF affects Mdm2 protein stability and p53 transactivation. *J Biol Chem.* 2001;10:10.
  - Yang CI, You L, Yeh CC, et al. Adenovirus-mediated p14(ARF) gene transfer in human mesothelioma cells. *J Natl Cancer Inst.* 2000;92:636–641.
  - Sweeney P, Pisters LL. AdCMVp53 gene therapy for locally advanced prostate cancer — where do we stand? *World J Urol.* 2000;18:121–124.
  - Swisher SG, Roth JA, Nemunaitis J, et al. Adenovirus-mediated p53 gene transfer in advanced non-small-cell lung cancer. *J Natl Cancer Inst.* 1999;91:763–771.
  - Swisher SG, Roth JA. Gene therapy in lung cancer. *Curr Oncol Rep.* 2000;2:64–70.
  - Nemunaitis J, Swisher SG, Timmons T, et al. Adenovirus-mediated p53 gene transfer in sequence with cisplatin to tumors of patients with non-small-cell lung cancer. *J Clin Oncol.* 2000;18:609–622.
  - Logothetis CJ, et al. AdCMV-p53 intraprostatic gene therapy preceding radical prostatectomy (RP): an *in vivo* model for targeted therapy development. *J Clin Oncol.* 1999;18:1020A.
  - Asai A, Miyagi Y, Sugiyama A, et al. Negative effects of wild-type p53 and s-Myc on cellular growth and tumorigenicity of glioma cells: Implication of the tumor suppressor genes for gene therapy. *J Neuro Oncol.* 1994;19:259–268.
  - Cui Z, Capoulade C, Moyret-Lalle C, et al. Resistance of MCF7 human breast carcinoma cells to TNF-induced cell death is associated with loss of p53 function. *Oncogene.* 1997;15:2817–2826.
  - Chen PL, Chen YM, Bookstein R, et al. Genetic mechanisms of tumor suppression by the human p53 gene. *Science.* 1990;250:1576–1580.
  - Johnson P, Gray D, Mowat M, et al. Expression of wild-type p53 is not compatible with continued growth of p53-negative tumor cells. *Mol Cell Biol.* 1991;11:1–11.
  - Lesoon-Wood LA, Kim WH, Kleinstein HK, et al. Systemic gene therapy with p53 reduces growth and metastasis of a malignant human breast cancer in nude mice. *Hum Gene Ther.* 1995;6:395–405.
  - Takahashi T, Carbone D, Nau MM, et al. Wild-type but not mutant p53 suppresses the growth of human lung cancer cells bearing multiple genetic lesions. *Cancer Res.* 1992;52:2340–2343.